Journal of Molecular Structure 1217 (2020) 128388

Contents lists available at ScienceDirect

Journal of Molecular Structure

journal homepage: http://www.elsevier.com/locate/molstruc

Comprehensive quantum mechanical studies on three bioactive anastrozole based triazole analogues and their SERS active graphene complex

Jamelah S. Al-Otaibi [a], Aljawhara H. Almuqrin [b], Y. Sheena Mary [c, *], Y. Shyma Mary [c]

[a] Department of Chemistry, College of Science, Princess Nourah Bint Abdulrahman University, Saudi Arabia
[b] Department of Physics, College of Science, Princess Nourah Bint Abdulrahman University, Saudi Arabia
[c] Department of Physics, Fatima Mata National College (Autonomous), Kollam, Kerala, India

ARTICLE INFO

Article history:
Received 14 January 2020
Received in revised form
23 April 2020
Accepted 4 May 2020
Available online 7 May 2020

Keywords:
DFT
Triazole
GERS
NLO
Docking
Graphene

ABSTRACT

Three triazole derivatives, 2-[3-(2-cyanopropan-2-yl)-5-(1,2,4-triazol-1-ylmethyl)phenyl]-2-methylpropanenitrile (anastrozole) (TR1), 3-amino-1-benzyl-5-phenyl-1H-1,2,4-triazole (TR2) and 5-amino-1-benzyl-3-phenyl-1H-1,2,4-triazole (TR3) were analyzed for the structural, nonlinear optical, electronic and biological properties. The functional nature of the compounds were analyzed using vibrational spectra and was compared with the scaled, simulated spectra obtained using DFT with diffused orbitals. Relaxed potential energy scan predicts the stable conformers. Frontier molecular orbital was found and used to generate some important data pertaining to the reactivity and stability of the molecule. Time dependent DFT was used to model the excitation and de-excitation dynamics of these molecules and to predict the use of these molecules as effective photo sensitizer in DSSC. This work further discusses in detail, NBO study for intra molecular interactions, MEP for reactivity preferences and hyperpolarizability calculations for predicting the optical properties. Further molecular docking studies were conducted for the compounds with CYP2C9 inhibitor (PDBID: 4NZ2), cytochrome P450 inhibitor (4D75), tyrosine-protein kinase JAK2 (4YTC), estragen synthase (4GL5) to predict their utility as potential. The compounds were found to interact with graphene monolayer results shows that there is enhancement in various physico-chemical descriptors and surface enhanced Raman spectra (SERS).

1. Introduction

Anastrozole is a newly developed benzyltriazole group non steroidal molecule, widely used against breast cancer, especially the hormone receptor positive breast cancer along with other chemotherapeutic agents [1]. It will reversibly bind with the aromatase enzyme by competitive inhibition, which enables the inhibition of the bioconversion of androgens to estrogens in the peripheral extra gonodal tissues like breast tissues [2], leading to about eighty five percent estradiol level without affecting the level of other corticosteroids [3]. Estrogen is a vital factor that promotes the growth and survival of young neoplastic cells, which binds to the estrogen receptors which enhances the cellular progression of the cancer by the production of several proteins required for the proliferation of cells [4]. Even though a variety of metabolotes are possible for this compound due to *N*-dealkylation, glucurodination and hydroxylation, the primary drug action is due to the unmetabolised anastrozole [5]. Anastrozole, an aromatase inhibitor is used with other treatments such as surgery or radiation to treat breast cancer in women and the side effect of this drug has been reported such as weakness, headache, weight gain, diarrhea, loss of apetite and depression [6]. Akcay and Bayrak [7] reported the computational studies of anastrozole and letrozole. Triazoles represent an important class of hetero-cyclic compounds having diverse biological properties such as anti-HIV activity [8,9], anti-microbial activity against gram positive bacteria [10], selective adrenergic receptor agonism [11]. Compounds containing triazole moiety are also found to have various industrial applications such as dyes, corrosion inhibition, photo stabilizers, photographic material and agrochemicals [12,13] together with their special catalytic behavior and magnetic properties [14]. Mary et al. [15] and Muthu et al. [16–18] reported computational and experimental study of triazole

* Corresponding author.
E-mail address: marysheena2018@rediffmail.com (Y.S. Mary).

https://doi.org/10.1016/j.molstruc.2020.128388
0022-2860/

derivatives. In the present work, spectroscopic characterization and molecular docking studies are reported for the triazole derivatives, 2-[3-(2-cyanopropan-2-yl)-5-(1,2,4-triazol-1-ylmethyl)phenyl]-2-methylpropanenitrile (TR1), 3-amino-1-benzyl-5-phenyl-1H-1,2,4-triazole (TR2) and 5-amino-1-benzyl-3-phenyl-1H-1,2,4-triazole (TR3). Quantum chemical studies for these molecules are not reported till date for these important analogues; hence we decided to perform detailed theoretical and computational analysis of these compounds. The DFT which is highly popular among the organic chemists has been used to carry out the study with B3LYP functional and the huge double diffused 6−311++G(d,p) basis set for improved accuracy. Relaxed potential energy scan (PES) of the molecules were performed to study the conformational preference of the compounds. Molecular properties of the title compounds have been calculated, including MEP, HOMO, LUMO, first and second order hyperpolarizability values. This paper also attempts the study of photovoltaic modeling of the triazole analogues with the help of TD-DFT using the long range effects corrected CAM-B3LYP orbital using the same basis sets for higher accuracy of the time dependent phenomena. By virtue of the molecule's biological activity molecular docking has also been studied and reported.

Graphene is one of the novel carbon allotropes with two dimensional structure and atomic thickness [19]. Chemical modification of graphene structures, reactions with organic and inorganic molecules and taking into account various noncovalent and covalent interactions with graphene are some techniques for functionalization of graphene [20–22]. The integration of graphene sheets with other functional parts is an effective way to boost their performance in a variety of applications [23]. Graphene quantum dots (GQDs) entered the field of uniqueness due to quantum containment and edge effects and these nano sized graphene fragments can be easily adsorbed by target molecules due to their large specific area [24]. Due to their efficient photoelectronic properties, graphene quantum dots can provide have stronger SERS signals to detect target molecules in solution [25,26]. Adsorption is an acceptable alternative for the various methods used to extract pollutants from drinking water due to its ease of operation and low cost. Nano based graphene materials are an appropriate alternative for removing critical contaminants from water due to their enhanced surface reactivity compared to their bulk counterparts [27–29]. Adsorption of molecules on carbon nano structures and graphene sheets can be a step in the development of nano sensing technology [30]. It is of common knowledge that graphene layer can be used to adsorb molecules. This may cause enhancement in Raman activity of the adsorbed molecules aiding the observation of surface enhanced Raman spectra (SERS) [31]. This manuscript examines the possibility of enhancement of Raman spectra of the compounds on adsorption at the surface of the graphene layer via various non covalent interactions.

2. Computational details

The ground state geometries of the compounds (Fig. 1) were simulated using the DFT method. The B3LYP hybrid functional [32,33] using 6−311++G(d,p) basis set were employed to perform the calculations in gas phase for all the above mentioned compounds in neutral state. The B3LYP functional is a popular density functional among chemists, which describes all the electronic properties of organic molecules in particular. The basis set used is comparatively large wit−h diffused functions to provide higher accuracy during the simulations [34]. The optimized structural parameters of DFT calculations and all other calculations at the same level of theory and basis set were used in the vibrational frequency calculations. Vibrational frequency calculations were performed with high degree of accuracy and no imaginary frequencies were found. The theoretically generated frequencies were scaled using a scaling factor of 0.9613 [35]. Relaxed potential energy scan were also performed using the same theory level. Electronic spectra and photovoltaic modeling was performed using long range corrected Coulomb-attenuating method introduced CAM-B3LYP using the same basis set. The calculations were performed for first six singlet states in methanol solvent cage using the IEFPCM solvation model [36]. Hence true minimum on the potential energy surface were obtained in each case. The Gaussview program [37] which is a graphical user interface designed to be used with Gaussian09 [38] has been used to predict the vibrational modes, intensities and spectra by visual animation for the verification of the normal mode assignments. The vibrational spectra of the title compounds are obtained from Spectrabase [39]. Dispersion corrected functionalω-B97XD along with the same basis sets was used to study the interaction of molecules with graphene layer [40].

3. Potential energy scan (PES)

PES (Fig.S1) was conducted to study the preference of conformation of the molecules, 2-[3-(2-cyanopropan-2-yl)-5-(1,2,4-triazol-1-ylmethyl)phenyl]-2-methylpropanenitrile (TR1), 3-amino-1-benzyl-5-phenyl-1H-1,2,4-triazole (TR2) and 5-amino-1-benzyl-3-phenyl-1H-1,2,4-triazole (TR3). Fully relaxed scan was conducted on the dihedral between the atoms of C13, C11, C14 and N1 at the scan interval of 30° from 0 to 180° using the B3LYP functional and 6−311++G(d,p) basis set for TR1. The global minima is observed at 60° as at that point, the heterocyclic ring is far away from the molecular plane, which is favored due to less amount of repulsion. The global maximum was at 120° as the heterocyclic ring is coming towards the central phenyl ring causing steric interaction

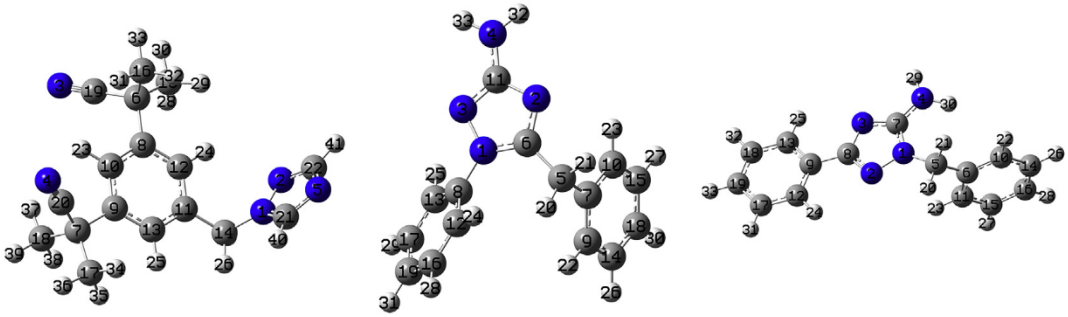

(a) (b) (c)

Fig. 1. Optimized geometry of (a) TR1 (b) TR2 (c) TR3.

due to van der Waal repulsion. Relaxed potential energy scan was conducted between the dihedrals 6C−5C−7C−10C along the C−N bond for 18 steps in the increment of 10° for TR2. The global minima is found to be at 60° where the substituent are in fully staggered conformation, while the global maxima was found to be at 0°, when the eclipsed conformation predominates and there is van der Waal's repulsion between the groups. In the case of TR3, the relaxed potential energy scans along the dihedrals of 2N−1N−5C−6C along the C−N single bond for 18 steps at an incremental angle of 10°. The global minima is found to be at 120° where the substituent are in fully staggered conformation, while the global maxima was found to be at 0°, where the C−N bond is in fully eclipsed conformation. The relative stabilization energy for the staggered form is 6.7864 kcal/mol.

4. Electronic properties and molecular electrostatic potential

HOMO and LUMO play an indispensable part in chemical reactions of compounds [41]. The frontier molecular orbitals, the density of states spectrum and UV spectra are given in Figs.S2-S4. The energies of HOMO, LUMO and energy gaps were found to be −8.657, −4.625, 4.032 eV for TR1, TR2 and TR3. Hardness(η), softness(σ), chemical potential(μ) and electrophlicity index(ω) are respectively, 2.016, 0.496, −6.641, 10.940 for TR1, 1.421, 0.704, −6.027, 12.784 for TR2 and 1.382, 0.724, −6.192, 13.875 for TR3. Following the above calculations, other electronic properties were summarized based on the relations shown in Table 1 [42]. The hardness value (reciprocal of softness) of the compound indicates that it cannot be polarized easily. The low softness value implies the low toxicity of the compound [43]. Further, the compound under study was found to have a good biological activity based on the electrophilicity index [44−47].

Data from electronic spectra (Table S1) can be used to model the photovoltaic efficiency of a compound. Organic compounds with specialized chromophores are capable of absorbing light and excite electrons to higher levels by vertical excitation. The excited electrons can transfer the electronic energy to the semiconducting photo electrode, which is usually made up of TiO2. If the energy of excited electrons are more than that of the band gap of the semiconductor, that energy can be transferred to the TiO2 to excite its electrons from valence band to conduction band. In the case of TiO2, the band gap is found to be −4.0 eV [48−50]. From these data, the free energy of electron injection can be found out, which is a measure of the spontaneity of the energy transfer between dye and semi conductor. The first major factor that decides the ability of the dye for vertical excitation is the light harvesting efficiency (LHE), which is a function of the oscillator strength (f) of the corresponding excitation. LHE is defined as $1\text{-}10^{-f}$, whose value changes from 0 to 1. For TR1 which contains a triazole ring and two cyano groups, the oscillator strength for the electronic transition at 207.06 nm is only 0.0132 and the LHE were found to be 0.0300, which is almost equal to zero. But for the compound TR2, the oscillator strength improved to 0.3015 for the 242.82 nm transition with an LHE of 0.5005, which indicates that 50% of the incident light energy can be used for electronic excitation and most interestingly, for the third derivative, TR3, the oscillator strength is 0.5847 for 239.11 nm excitation, whose LHE is 0.7298, which means roughly 73% of the incident light energy can be used for electronic excitations. The ΔG_{inject} in kcal/mol is −35.697,-42.823 and −43.031 kcal/mol respectively for the three derivatives, which shows that the substituted derivatives can effectively act as a better photo sensitizer than the parent TR1 [51]. This also indicated that the photovoltaic efficiency of dyes can be tuned.

Molecular electrostatic potential (MEP) gives a clear picture of distribution of charge at surface and surrounding of the title compound in three dimensions. By doing so, the nature of interactions and chemical bonds can be identified. Color grading helps us to classify nucleophilic and electrophilic regions effortlessly. It also aids in evaluating the physiochemical properties of the title compound [52,53]. Fig.S5 shows the MEP map for the title compounds. Color grading (Red, Orange, Yellow, Green, Blue in the increasing order) is used. N atom has the highest electrophilicity indicated by red color, while hydrogen atoms have the highest nucleophilicity. Neutral regions are shown in green.

5. Nonlinear optical properties

Properties like the first order hyperpolarizability, polarisability and dipole moment of the title compound were studied. These parameters help us to understand the non-linear optical nature of the compound [54], which in utility for the design of a variety of organic electronic devices. Urea was chosen to compare the results obtained as it is the classical NLO material. It can be seen that the TR2 has higher first-order hyperpolarizability (1.219×10^{-30} e.s.u) and TR1 has lower value and in comparison to that of Urea, these values are respectively 9.38, 49.09, 17.13 times that of urea indicating the likely NLO candidature [55,56]. The second order hyperpolarizability varies in the order TR1 > TR3 > TR2 (table S3).

6. Molecular docking

Sub-atomic docking was utilized to perceive the dynamic site of the receptor, and secure the best geometry of ligand-receptor complex. Prediction of Activity Spectra [57] predicts different types of activities and given in Table S3. The high resolution crystal structure of corresponding receptors CYP2C9 inhibitor (PDBID: 4NZ2), cytochrome P450 inhibitor (4D75), tyrosine-protein kinase JAK2 (4YTC), estragen synthase (4GL5) were downloaded from the RCSB protein data bank website. Several genetic polymorphisms in genes such as cytochrome-P450 (CYP)2C8 and CYP2C9, may influence survival after cancer diagnosis due to their role in the metabolism of various breast cancer drugs, including tamoxifen and chemotherapy [58,59]. Cytochrome P450s (CYPs) have been to a great extent neglected in malignancy tranquilize advancement, recognized uniquely for their job in stage I digestion of chemotherapeutics. The principal effective system focusing on CYP compounds in malignancy treatment was the advancement of strong inhibitors of CYP19 (aromatase) for the treatment of bosom disease

Table 1
Chemical descriptors.

Molecule	E_H	E_L	$I = -E_H$	$A = -E_L$	Gap	η	Σ	X	μ	ω	ε
TR1	−8.657	−4.625	8.657	4.625	4.031	2.016	0.496	6.641	−6.641	10.940	0.091
TR2	−7.447	−4.606	7.477	4.606	2.841	1.421	0.704	6.027	−6.027	12.784	0.078
TR3	−7.574	−4.810	7.574	4.810	2.763	1.382	0.724	6.192	−6.192	13.875	0.072
TR1-G	−8.663	−5.726	8.663	5.726	2.937	1.469	0.681	7.195	−7.195	17.621	0.057
TR2-G	−7.456	−5.726	7.456	5.726	1.730	0.865	1.156	6.591	−6.591	25.112	0.040
TR3-G	−7.575	−5.725	7.575	5.725	1.850	0.925	1.081	6.650	−6.650	23.910	0.042

[60]. Tyrosine-protein kinase JAK2, a cytoplasmic tyrosine kinase, plays a critical role in hematopoiesis and activating mutations in this kinase are associated with a number of hematological disorders [61]. A definitive objective of bosom malignancy therapeutics for example to recognize and hinder a basic advertiser of carcinogenesis, anticipation, and to distinguish and square basic endurance pathways, treatment has effectively been accomplished by misusing information on the estrogen (E2)/estrogen receptor (ER) signal transduction framework [62]. All molecular docking calculations were performed on AutoDock4.2 [63], Auto Dock-Vina software [64,65] and as reported in literature [66,67].

The ligand binds at the active site of the substrates with the aid of weak non-covalent interactions (NCI) as detailed in Table S4 and Fig.S6. The docked ligand forms a stable complex with the receptors as depicted in Fig.S7. The binding free energy value of ligand with substrate CYP2C9 inhibitor, cytochrome P450 inhibitor, tyrosine-protein kinase JAK2, estrogen synthase are −6.6, −9.8, −6.6, −6.8 kcal/mol for TR1, -8.5, −8.3, −7.7, −7.5 TR2 and -8.3, −8.4, −7.5, −7.7 for TR3 (table S4). These preliminary results suggest that the compound having inhibitory activity against the receptors.

7. Natural bond orbital (NBO) analysis

NBO's is widely used to determine the electron density location in the atoms in the molecules and also in the chemical bonds between the atoms in a molecule. For the molecules under study, NBO analysis was performed using the NBO package incorporated in the Gaussian09 software [68,69]. The charge transfer from donor to acceptor orbitals results from increasing stabilization energy. The second order Fock matrix was used for the determination of the donor acceptor interactions. The important interactions are: N1→π*(N5−C21), N1→π*(N2−C22), N3→σ*(C6−C19), N4→σ*(C7−C20), N2−C22→π*(N5−C21), N5−C21→π*(N2−C22), C8−C12→π*(C9−C10), C8−C12→π*(C11−C13), C9−C10→π*(C8−C12), C9−C10→π*(C11−C13), C11−C13→π*(C8−C12), C11−C13→π*(C9−C10) with energies, 50.82, 25.25, 12.00, 12.04, 11.30, 30.00, 19.85, 22.50, 20.83, 20.21, 19.06, 20.97 kcal/mol for TR1; N1→π*(N2−C6), N4→π*(N3−C11), N2−C6→π*(N3−C11), C8−C12→π*(C13−C17), C8−C12→π*(C16−C19), N1→π*(N3−C11), N1→π*(C8−C12) with energies, 58.81, 56.43, 31.09, 19.19, 19.95, 18.50, 15.03 kcal/mol for TR2 and N1→π*(N2−C8), N1→π*(N3−C7), N4→σ*(N7−C7) with energies, 21.11, 57.29, 49.31 kcal/mol for TR3. The interaction between the orbitals cause the intra-molecular charge transfer provided the extra stabilization energy to system. The lone pair charge transfer provided the highest stabilization energy to the system.

8. Vibrational spectra

The C−H stretching modes are in the region 3000-3100 cm^{-1} (table S5) and the frequencies calculated at the range 3208−3077 cm^{-1}, 3122-3065 cm^{-1} and 3103-3058 cm^{-1} belongs to TR1, TR2 and TR3 aromatic stretching vibrations [70,71]. Experimental aromatic CH stretching vibrations are observed at 3125, 3096, 3060 cm^{-1} (IR), 3205, 3130, 3075 cm^{-1} (Raman) (TR1), 3135, 3095, 3058 cm^{-1} (IR) (TR2) and at 3100, 3050 cm^{-1} (IR) (TR3). The δC-H were observed at 1220, 1145, 1140 cm^{-1} (IR), 1200, 1147, 1137 cm^{-1} (Raman), 1212, 1142, 1141 cm^{-1} (DFT) for TR1, 1175, 1158, 1080, 1020 cm^{-1} (IR), 1175, 1160, 1081, 1019 cm^{-1} (DFT) for TR2 and at 1195, 1175, 1122, 1097, 1075, 1024 cm^{-1} (IR), 1192, 1127, 1120, 1093, 1076, 1023 cm^{-1} (DFT) for TR3. Methyl modes are assigned at 3040, 2948 cm^{-1} (IR), 3045, 3025, 2935 cm^{-1} (DFT) (stretching); 1495-950 cm^{-1} (IR), 1500-950 cm^{-1} (Raman), 1492-949 cm^{-1} (DFT) (bending modes) for TR1; NH2 modes at: 3450, 1625, 1070 cm^{-1} (IR) for TR2 and at 3450, 1640 cm^{-1} (IR) for TR3. The CH2 modes are observed at 2975, 1350, 860, 752 cm^{-1} (IR), 3005, 2970, 1350, 758 cm^{-1} (Raman), 3015-754 cm^{-1} (DDFT) for TR1, 3010, 2950, 1462, 1355, 1295, 785 cm^{-1} (IR), 3018-797 cm^{-1} (DFT) for TR2 and at 2950, 1362, 1308, 725 cm^{-1} (IR), 2935-722 cm^{-1} (DFT) for TR3. Usually, C≡N cyanide vibrations are observed at 2250 cm^{-1} and in our study, it is at 2225 cm^{-1} (IR), 2230 cm^{-1} (Raman), 2211, 2210 cm^{-1} (DFT) for TR1 [72,73]. Beegum et al. [73] reported C≡N stretching modes at 2238, 2245 cm^{-1} in the IR spectrum, 2262, 2247 cm^{-1} in the Raman spectrum and at 2257 cm^{-1} theoretically. The triazole CN and NN stretching modes are assigned at 1300, 1272, 979 cm^{-1} (IR), 1300, 1271 cm^{-1} (Raman), 1301, 1269, 981 cm^{-1} (DFT) for TR1, 1555, 1475, 1405, 1342, 1008 cm^{-1} (IR), 1556, 1475, 1404, 1344, 1011 cm^{-1} (DFT) for TR2 and at 1568, 1440, 1410, 1344, 1287, 1000 cm^{-1} (IR), 1569, 1442, 1418, 1346, 1289, 998 cm^{-1} (DFT) for TR3 [15]. Mary et al. reported the *N*−N stretching modes at 939, 944 and 956 cm^{-1} theoretically [44] and the CN stretching modes at 1577, 1330, 1250 (IR), 1579, 1218 (Raman), 1579, 1325, 1243, 1214 (DFT) [15].

9. Adsorption behavior of molecules on the surface of graphene

Graphene, which is a monolayer of graphite is an ideal candidate to study the surface interaction properties of the molecules under study. This interaction can be easily analyzed using Surface enhanced Raman spectroscopy (SERS) methods [74–76] and analysis of Raman spectra of pyridine on silver was reported [77]. SERS is found to enhance the signal strength of even weak Raman scattering signals of small molecules [78,79] and this unique property helps in the search for novel active materials, sensors etc with extremely high accuracy, uniformity and reproducibility. Graphene [80] a 2D sheet of carbon molecules show amazing Raman dispersing properties when contrasted with respectable metals because of its high adsorptivity, concoction soundness, biocompatibility alongside novel electronic and phonon properties. Graphene upgraded Raman dissipating (GERS) utilize graphene as a substrate rather than metal surfaces. Graphene related materials like graphene oxide [81,82], aged and nanomesh graphene [83,84] and graphene quantum dots are used as substrate for SERS applications [85].

In our work, we investigate electronic and vibrational properties of the compounds over graphene quantum dots. The adsorption energy (Ead) of the title compound over graphene is calculated using the following equation: $E_{ad} = E_{titlecompound+graphene} - (E_{titlecompound} + E_{graphene})$ where $E_{titlecompound+graphene}$ is the optimized total energy of title compound over graphene, $E_{titlecompound}$ is the optimized energy of title compound and $E_{graphene}$ the optimized energy of graphene [86]. Also the enhancement factors are calculated according to literature [86]. Using the definition, negative value of E_{ad} value shows a stable adsorption complex on the graphene. The Raman spectra of the title compounds adsorbed in graphene, HOMO-LUMO and MEP plots are given in Figs. S8-S10. Table 1 provides data of the various electron density descriptors of the graphene adsorbed TR1, TR2 and TR3. Chemical potential value is more negative for TR1-G (−7.195 eV), which means that this system is chemically more stable. High ionization energy values and high energy gap confirms this observation. It may be due to the presence of electron withdrawing cyano groups in TR1, adsorption is high over electron rich graphene layer. Table S2 indicates that there is a tremendous increase in the non linear optical activity of the compounds when they are adsorbed over the graphene and forms a complex. All the related properties like polarisability and first and second order hyperpolarizability values increased dramatically. The trend in adsorption energy of the molecules over

graphene is given in Table S6. The adsorption energy is maximum for TR2-G complex (−4.64 kcal/mol) and the least is for TR3-G complex which is due to electronegative nature of atoms in TR2-G as evident from molecular electrostatic potential maps and frontier molecular orbitals of TR2-G complex [86].

GERS data (Table S7) shows enhancement of Raman signals for several wave numbers. For TR1, the significant enhancement is at 1352 cm^{-1} from 0.35 to 55.15, whose relative enhancement factor is 15657, which is easily detectable. It corresponds to the δCH2 vibration. Also enhancement of 1792 and 1076 times are observed for 3095 and 1593 cm^{-1}, which corresponds to υCH and υPh vibrations. In the case of TR2, significant Raman enhancement of 1659 times was observed for δCH2 vibrations at 1353 cm^{-1}. In the case of TR3, an enhancement factor of 6285 is observed at 1346 cm^{-1}, which corresponds to υCN vibration. This indicates that GERS using graphene can be used for the detection of these compounds in various medium and Graphene can act as an easily detectable and cost effective sensor for this.

10. Conclusion

The compounds have been characterized using FT-IR and FT-Raman and UV−Vis spectroscopic techniques. The experimental and theoretical results were found to be in harmony. Relaxed potential energy scan showed the conformational preference of the molecules are in consistent with the optimized geometry. FMO's predicts the various physico-chemical properties of the molecules. Study of the MESP predicted the electrophilic and nucleophilic centers for the compounds. The ability of the molecules to be used as photo sensitizers in DSSC's are also appreciable. Hyperpolarizability calculations show that all the molecules are effective candidates to be used in NLO applications. The title molecules are docked with receptors CYP2C9 inhibitor (PDBID: 4NZ2), cytochrome P450 inhibitor (4D75), tyrosine-protein kinase JAK2 (4YTC), estragen synthase (4GL5) and gives good binding affinity values. Adsorption on graphene tremendously alters the physico-chemical profile of the compounds. It enhances the non linear optical properties and the Raman enhancement observed from GERS simulation indicates the utility of grahene as potential sensors for detection in condensed phase.

Author contribution statement

All authors conceived and designed the calculations. Analyzed and interpreted the data; contributed materials, analysis tools or data and software; wrote the paper.

Declaration of competing interest

The authors declare no conflict of interest.

Acknowledgements

The authors would like to thank the Center for Promising Research in Social Research and Women's Studies Deanship of Scientific Research, at Nourah bint Abdulrahman University for funding this Project in 2020.

Appendix A. Supplementary data

Supplementary data related to this article can be found at https://doi.org/10.1016/j.molstruc.2020.128388.

References

[1] C. Nantasenamat, A. Worachartcheewan, S. Prachayasittikul, C. Isarankura-Na-Ayudhya, V. Prachayasittikul, QSAR modeling of aromatase inhibitory activity of 1-substituted 1,2,3-triazole analogs of letrozole, Eur. J. Med. Chem. 69 (2013) 99−114.
[2] S. Mirzaie, L. Chupani, E.B. Asadabadi, A.R. Shahverdi, M. Jamalan, Novel inhibitor discovery against aromatase through virtual screening and molecular dynamic simulation: a computational approach in drug design, EXCLI J 12 (2013) 168−183.
[3] J. Russo, M.H. Lareef, G. Balogh, S. Guo, I.H. Russo, Estrogen and its metabolites arecarcinogenic agents in human breast epithelial cells, J. Steroid Biochem. Mol. Biol. 87 (2003) 1−25.
[4] A. Eisen, M. Trudeau, W. Shelley, H. Messersmith, K.I. Pritchard, Aromatase inhibitors in adjuvant therapy for hormone receptor positive breast cancer: a systematic review, Canc. Treat Rev. 34 (2008) 157−174.
[5] R.J. Santen, S. Santner, B. Davis, J. Veldhuis, E. Samojlik, E. Ruby, Amino glutethimide inhibits extra glandular estrogen productionin post menopausal women with breast carcinoma, J. Clin. Endocrinol. Metab. 47 (1978) 1257−1265.
[6] J.M. Nabholtz, A. Buzdar, M. Pollak, W. Harwin, G. Burton, A. Manglik, M. Steinberg, A. Webster, M. Von Euler, Anastrozole is superior to tamoxifen as first line therapy for advanced breast cancer in post menopausal women, results of a north American multicenter randomized trial, J. Clin. Oncol. 18 (2000) 3758−3767.
[7] H.T. Akcay, R. Bayrak, Computational studies on the abastrozole and letrozole, effective chemotherapy drugs against breast cancer, Spectrochim. Acta 122 (2014) 142−152.
[8] C.W. Tornoe, C. Christensen, M. Meldal, Peptidotriazoles on solid phase: [1,2,3]-triazoles by regiospecific copper(I)-catalyzed 1,3-dipolar cycloadditions of terminal alkynes to azides, J. Org. Chem. 67 (2002) 3057−3064.
[9] H. Lazrek, M. Taourirte, T. Oulih, J. Barascut, J. Imbach, C. Pannecouque, M. Witrouw, E. De Clercq, Synthesis and anti-HIV activity of new modified 1,2,3-triazole acycylonucleosides, Nucleos Nucleot. Nucleic Acids 20 (2001) 1949−1960.
[10] R. Alvarez, S. Velazquez, A. San-Felix, S. Aquaro, E. De Clercq, C.F. Perno, A. Karlsson, J. Balzarini, M.J. Camarasa, 1,2,3-triazole-[2,5-bis-O-(tert-butyldimethylsilyl)-β-D-ribofuranosyl]-3'-spiro-5"-(4"-amino-1",2"-oxathiloe 2"-2"-dioxide)(TSAO) analogs: synthesis and anti-HIV-1 activity, J. Med. Chem. 37 (1994) 4185−4194.
[11] S. Velazquez, R. Alvarez, C. Perez, F. Gago, E. De Clercq, J. Balzarini, M.J. Camarasa, Regiospeific synthesis and anti-human immunodeficiency virus activity of novel 5-substituted N-alkylcarbamoyl and N,N-dialkyl carbamoyl 1,2,3-triazole-TSAO analogues, Antivir. Chem. Chemother. 9 (1998) 481−489.
[12] Y. Peng, B. Li, J. Zhou, B. Li, Y. Zhang, Synthesis and crystal structure of 1,4-bis(1H-1,2,4-triazol-1-methyl)benzene, Chin. J. Struct. Chem. 23 (2004) 985−988.
[13] B. Wang, N. Liu, C. Shao, Q. Zhang, X. Wang, Y. Hu, Preparation of 1,4,5-trisubstituted 5-acyl-1,2,3-triazoles by selective acylation between copper(I)-carbon(sp) and copper(I)-carbon(sp^2) bonds with acyl chlorides, Adv. Synth. Catal. 355 (2013) 2564−2568.
[14] L. Xie, G. Liu, Y. Wang, J.D. Wang, J.F. Chen, Synthesis, crystal structure and quantum chemical investigation of bis-Schiff base compounds derived from 2-phenyl-1,2,3-triazole-4-carboxaldehyde with diamine, Chin. J. Struct. Chem. 27 (2008) 616−621.
[15] Y.S. Mary, F.A.M. Al-Omary, G.A.E. Mostafa, A.A. El-Emam, P.S. Manjula, B.K. Sarojini, B. Narayana, S. Armakovic, S.J. Armakovic, C. Van Alsenoy, Insight into the reactive properties of newly synthesized 1,2,4-triazole derivative by combined experimental (FT-IR and FT-Raman) and theoretical (DFT and MD) study, J. Mol. Struct. 1141 (2017) 542−550.
[16] N.R. Sheela, S. Muthu, S. Sampathkrishnan, Molecular orbital studies (hardness, chemical potential and electrophilicity), vibrational investigation and theoretical NBO analysis of 4-4'-(1H-1,2,4-triazol-1-yl methylene)dibenzonitrile based on ab initio and DFT methods, Spectrochim. Acta 120 (2014) 237−251.
[17] T.K. Kuruvilla, J.C. Prasana, S. Muthu, J. George, Vibrational spectroscopic (FT-IR, FT- Raman) and quantum mechanical study of 4-(2-chlorophenyl)-2-ethyl-9-methyl-6H-thieno[3,2-f][1,2,4]triazolo[4,3-a[1,4]diazepine, J. Mol. Struct. 1157 (2018) 519−529.
[18] S. Muthu, M. Prasathy, R.A. Balaji, Experimental and theoretical investigations of spectroscopic properties of 8-chloro-1-methyl-6-phenyl-4H-[1,2,4]triazolo [4,3-a][1,4]benzodiazepine, Spectrochim, Acta 106 (2013) 129−145.
[19] M. Rouhani, DFT study on adsorbing and detecting possibility of cyanogens chloride by pristine, B, Al, Ga, Si and Ge doped graphene, J. Mol. Struct. 1181 (2019) 518−535.
[20] Q.H. Wang, M.C. Hersam, Room temperature molecular resolution characterization of self assembled organic monolayers on epitaxial graphene, Nat. Chem. 1 (2009) 206−211.
[21] Y. Si, E.T. Samulski, Synthesis of water soluble graphene, Nano Lett. 8 (2008) 1679−1682.
[22] A. Bostwick, T. Ohta, T. Seyller, K. Horn, E. Rotenberg, Quasiparticle dynamics in graphene, Nat. Phys. 3 (2007) 36−40.
[23] J. Park, S.B. Jo, Y.J. Yu, Y. Kim, J.W. Yang, W.H. Lee, H.H. Kim, B.H. Hong, P. Kim,

K. Cho, K.S. Kim, Single gate band gap opening of bilayer graphene by dual molecular doping, Adv. Mater. 24 (2012) 407–411.
[24] H. Cheng, Y. Zhao, Y. Fan, X. Xie, L. Qu, G. Shi, Graphene quantum dot assembled nanotubes: a new platform for efficient Raman enhancement, ACS Nano 6 (2012) 2237–2244.
[25] W. Xu, N. Mao, J. Zhang, Graphene: a platform for surface enhanced Raman spectroscopy, Small 9 (2013) 1206–1224.
[26] M. Bacon, S.J. Bradley, T. Nann, Graphene quantum dots, Part. Part. Syst. Char. 31 (2014) 415–428.
[27] L.S. Mandeep, R. Kakkar, DFT study on the adsorption of p-nitrophenol over vacancy and Pt-doped graphene sheets, Comput. Theor. Chem. 1142 (2018) 88–96.
[28] A.S. Rad, E. Sani, E. Binaeian, M. Peyravi, M. Jahanshahi, DFT study on the adsorption of diethyl, ethyl methyl and dimethyl ethers on the surface of gallium doped graphene, Appl. Surf. Sci. 401 (2017) 156–161.
[29] L.S. Mandeep, R. Kakkar, Adsorption of bromonitromethane over graphene based substrates, a density functional theory analysis, Chem. Select. 4 (2019) 4967–4974.
[30] C. Thierfelder, M. Witte, S. Blankenburg, E. Rauls, W.G. Schmidt, Methane adsorption on graphene from first principles including dispersion interaction, Surf. Sci. 605 (2011) 746–749.
[31] Y. Jiang, J. Wang, L. Malfatti, D. Carboni, N. Senes, P. Innocenzi, Highly durable graphene-mediated surface enhanced Raman scattering (G-SERS) nano composites for molecular detection, Appl. Surf. Sci. 450 (2018) 451–460.
[32] A.D. Becke, Density functional thermo chemistry. III. The role of exact exchange, J. Chem. Phys. 98 (1993) 5648–5652.
[33] C. Lee, W. Yang, R.G. Parr, Development of the Colle-Salvetti correlation energy formula into a functional of the electron density, Phys. Rev. B37 (1988) 785–789.
[34] A.D. Becke, Density functional exchange energy approximation with correct asymptotic behavior, Phys. Rev. A38 (1988) 3098–3100.
[35] J.B. Foresman, E. Frisch, Exploring Chemistry with Electronic Structure Methods: A Guide to Using Gaussian, Pittsburg, 1996. PA.
[36] J.S. Al-Otaibi, Y.S. Mary, Y.S. Mary, R. Thomas, Quantum mechanical and photovoltaic studies on the cocrystals of hydrochlorothiazide with isonazid and malonamide, J. Mol. Struct. 1197 (2019) 719–726.
[37] T. Keith, J. Millam, Gaussview 5, Semichem. Inc. Shawnee Mission KS, 2009.
[38] M.J. Frisch, G.W. Trucks, H.B. Schlegel, G.E. Scuseria, M.A. Robb, J.R. Cheeseman, G. Scalmani, V. Barone, B. Mennucci, G.A. Petersson, H. Nakatsuji, M. Caricato, X. Li, H.P. Hratchian, A.F. Izmaylov, J. Bloino, G. Zheng, J.L. Sonnenberg, M. Hada, M. Ehara, K. Toyota, R. Fukuda, J. Hasegawa, M. Ishida, T. Nakajima, Y. Honda, O. Kitao, H. Nakai, T. Vreven, J.A. Montgomery Jr., J.E. Peralta, F. Ogliaro, M. Bearpark, J.J. Heyd, E. Brothers, K.N. Kudin, V.N. Staroverov, T. Keith, R. Kobayashi, J. Normand, K. Raghavachari, A. Rendell, J.C. Burant, S.S. Iyengar, J. Tomasi, M. Cossi, N. Rega, J.M. Millam, M. Klene, J.E. Knox, J.B. Cross, V. Bakken, C. Adamo, J. Jaramillo, R. Gomperts, R.E. Stratmann, O. Yazyev, A.J. Austin, R. Cammi, C. Pomelli, J.W. Ochterski, R.L. Martin, K. Morokuma, V.G. Zakrzewski, G.A. Voth, P. Salvador, J.J. Dannenberg, S. Dapprich, A.D. Daniels, O. Farkas, J.B. Foresman, J.V. Ortiz, J. Cioslowski, D.J. Fox, Gaussian 09, Revision B.01, Gaussian, Inc., Wallingford CT, 2010.
[39] Bio-rad laboratories, inc., SpectraBase. http://spectrabase.com/.
[40] J.-D. Chai, M. Head-Gordon, Long-range corrected hybrid density functionals with damped atom-atom dispersion corrections, Phys. Chem. Chem. Phys. 10 (2008) 6615–6620.
[41] K. Fukui, Science vol. 218 (1982) 747–754. The Role of Frontier Orbitals in Chemical Reactions.
[42] R.G. Parr, R.A. Donnelly, M. Levy, W.E. Palke, Electronegativity: the density functional viewpoint, J. Chem. Phys. 68 (1988) 3801–3807.
[43] Y.S. Mary, H.T. Varghese, C.Y. Panicker, M. Girisha, B.K. Sagar, H.S. Yathirajan, A.A. Al-Saadi, C. Van Alsenoy, Vibrational spectra, HOMO, LUMO, NBO, MEP analysis and molecular docking study of 2,2-diphenyl-4-piperidin-1-yl)butanamide, Spectrochim. Acta 150 (2015) 543–556.
[44] Y.S. Mary, P.B. Miniyar, Y.S. Mary, K.S. Resmi, C.Y. Panicker, S. Aramkovic, S.J. Armakovic, R. Thomas, B. Sureshkumar, Synthesis and spectroscopic study of three new oxadiazole derivatives with detailed computational evaluation of their reactivity and pharmaceutical potential, J. Mol. Struct. 1173 (2018) 469–480.
[45] R.M. LoPachin, T. Gavin, A. De Caprio, D.S. Barber, Application of the hard and soft, acids and bases (HSAB) theory to toxicant-target interactions, Chem. Res. Toxicol. 25 (2012) 239–251.
[46] H. Xu, D.C. Xu, Y. Wang, Natural indices for the chemical hardness/softness of metal cations and ligands, ACS Omega 2 (2017) 7185–7193.
[47] R.M. LoPachin, T. Gavin, Reactions of electrophiles with nucleophilic thiolate sites: relevance to pathophysiological mechanisms and remediation, Free Radic. Res. 50 (2016) 195–205.
[48] L. Louazri, A. Amine, S.M. Bouzzine, M. Hamidi, M. Bouachrine, Photovoltaic properties of Zn-complexed-phtalocyanine and derivatives for DSSCs application, J. Mater. Environ. Sci. 7 (2016) 2305–2313.
[49] X.F. Ren, J. Zhang, G.J. Kang, Theoretical studies of electronic structure and photophysical properties of a series of indoline dyes with triphenylamine ligand, J. Nanomater. (2015), https://doi.org/10.1155/2015/605728. Article ID: 605727.
[50] K. Chaitanya, X.H. Ju, B.M. Heron, Can elongation of the π-system in triarylamine derivated sensitizers with either benzothiadiazole and/or ortho-fluorophenyl moieties enrich their light harvesting efficiency? – a theoretical study, RSC Adv. 5 (2015) 3978–3998.
[51] Y.S. Mary, T. Ertan-Bolelli, R. Thomas, A.R. Krishnan, K. Bolelli, E.N. Kasap, T. Onkol, I. Yildiz, Quantum mechanical studies of three aromatic halogen-substituted bioactive sulfonamidobenzoxazole compounds with potential light harvesting properties, Polycycl. Aromat. Comp., https://doi.org/10.1080/10406638.2019.1689405.
[52] J.S. Murry, K. Sen, Molecular Electrostatic Potential Concepts and Applications, Elsevier, Amesterdam, 1996.
[53] B. Sureshkumar, Y.S. Mary, C.Y. Panicker, S. Suma, S. Armakovic, S.J. Armakovic, C.Van Alsenoy, B.Narayana, Quinoline derivatives as possible lead compounds for anti-malarial drugs: Spectroscopic, DFT and MD study, Arabian Journal of Chemistry, https://doi.org/10.1016/j.arabjc.2017.07.006.
[54] S.R. Sheeja, N.A. Mangalam, M.R.P. Kurup, Y.S. Mary, K. Raju, H.T. Varghese, C.Y. Panicker, Vibrational spectroscopic studies and computational study of quinoline-2-carbaldehyde benzoyl hydrazone, J. Mol. Struct. 973 (2010) 36–46.
[55] J.S.P.P. Leela, R. Hemamalini, S. Muthu, A.A. Al-Saadi, Spectroscopic investigation (FTIR spectrum), NBO, HOMO-LUMO energies , NLO and thermodynamic properties of 8-methyl-N-vanillyl-6-nonenamide by DFT methods, Spectrochim. Acta 146 (2015) 177–186.
[56] C.Y. Panicker, H.T. Varghese, K.C. Mariamma, K. John, S. Mathew, J. Vinsova, C. Van Alsenoy, Y.S. Mary, Spectroscopic investigations and computational study of 2-[acetyl-(4-bromophenyl)carbamoyl]-4-chlorophenyl acetate, J. Raman Spectrosc. 6 (2010) 707–716.
[57] A. Lagunin, A. Stepanchikova, D. Filimonov, V. Poroikov, PASS: prediction of activity spectra for biologically active substances, Bioinformatics 16 (2000) 747–748.
[58] Y. Jin, Z. Desta, V. Stearns, B. Ward, H. Ho, K.H. Lee, T. Skaar, A.M. Storniolo, L. Li, A. Araba, R. Blanchard, A. Nguyen, L. Ullmer, J. Hayden, S. Lemler, R.M. Weinshilboum, J.M. Rae, D.F. Hayes, D.A. Flockhart, CYP2D6 genotype, antidepressant use, and tamoxifen metabolism during adjuvant breast cancer treatment, J. Natl. Cancer Inst. 97 (2005) 30–39.
[59] H. Jernström, E. Bågeman, C. Rose, P.E. Jonsson, C. Ingvar, CYP2C8 and CYP2C9 polymorphisms in relation to tumour characteristics and early breast cancer related events among 652 breast cancer patients, BJC (Br. J. Cancer) 101 (2009) 1817–1823.
[60] R.D. Bruno, V.C. Njar, Targeting cytochrome P450 enzymes: a new approach in anti- cancer drug development, Bioorg. Med. Chem. 15 (2007) 5047–5060.
[61] A. Majumder, P. Sayeski, Tyrosine-protein kinase JAK2 inhibitors for the treatment of myeloproliferative neoplasms, Drugs Future 35 (2010) 651, https://doi.org/10.1358/dof.2010.035.08.1514131.
[62] R. Lupu, J.A. Menendez, Targeting fatty acid synthase in breast and endometrial cancer: an alternative to selective estrogen receptor modulators? Endocrinology 147 (2006) 4056–4066.
[63] G.M. Morris, R. Huey, W. Lindstrom, M.F. Sanner, R.K. Belew, D.S. Goodsell, A.J. Olson, Autodock4 and AutoDockTools4: automated docking with selective receptor flexibility, J. Comput. Chem. 16 (2009) 2785–2791.
[64] O. Trott, A.J. Olson, AutoDockVina: improving the speed and accuracy of docking with a new scoring function, efficient optimization, J. Comput. Chem. 31 (2010) 455–461.
[65] G.M. Morris, D.S. Goodsell, R.S. Halliday, R. Huey, W.E. Hart, R. Belew, A.J. Olson, Automated docking using a Lamarckian genetic algorithm and an empirical binding free energy function, J. Comput. Chem. 19 (1998) 1639–1662.
[66] Y.S. Mary, C.Y. Panicker, M. Sapnakumari, B. Narayana, B.K. Sarojini, A.A. Al-Saadi, C. Van Alsenoy, J.A. War, , F.T.-I.R., NBO, HOMO-LUMO, MEP analysis and molecular docking study of 1-]3-(4-fluorophenyl)-5-phenyl-4,5-dihydro-1H-pyrazol-1-yl]ethanone, Spectrochim, Acta 136 (2015) 483–493.
[67] Y.S. Mary, Y.S. Mary, R. Thomas, B. Narayana, S. Samshuddin, B.K. Sarojini, S. Armakovic, S.J. Armakovic, G.G. Pillai, Theoretical studies on the structure and various physic-chemical and biological properties of a terphenyl derivative with immense anti-protozoan activity, Polycycl. Aromat. Comp.. https://doi.org/10.1080/10406638.2019.1624974.
[68] E.D. Glendening, A.E. Reed, J.E. Carpenter, F. Weinhold, NBO Version 3.1, Gaussian Inc., Pittsburgh, PA, 2003.
[69] Y.S. Mary, H.T. Varghese, C.Y. Panicker, M. Girisha, B.K. Sagar, H.S. Yathirajan, A.A. Al-Saadi, C. VanAlsenoy, Vibrational spectra, HOMO, LUMO, NBO, MEP analysis and molecular docking study of 2,2-diphenyl-4-(piperidin-1-yl) butanamide, Spectrochim. Acta 150 (2015) 543–556.
[70] N.P.G. Roeges, A Guide to the Complete Interpretation of Infrared Spectra of Organic Structures, John Wiley and Sons Inc., New York, 1994.
[71] A. Chandran, H.T. Varghese, Y.S. Mary, C.Y. Panicker, T.K. Manojkumar, C. Van Alsenoy, G. Rajendran, F.T.-I.R., FT-Raman and computational study of (E)-N-carbamimidoyl-4-((4-methoxybenzylidene)amino)benzenesulfonamide, Spectrochim. Acta 92 (2012) 84–90.
[72] S. Beegum, Y.S. Mary, H.T. Varghese, C.Y. Panicker, S. Armakovic, S.J. Armakovic, J. Zitko, M. Dolezal, C. Van Alsenoy, Vibrational spectroscopic analysis of cyanopyrazine-2-carboxamide derivatives and investigation of their reactive properties by DFT calculations and molecular dynamics simulations, J. Mol. Struct. 1131 (2017) 1–15.
[73] S. Beegum, Y.S. Mary, Y.S. Mary, R. Thomas, S. Armakovic, S.J. Armakovic, J. Zitko, M. Dolezal, C. Van Alsenoy, Exploring the detailed spectroscopic characteristics, chemical and biological activity of two cyanopyrazine-2-carboxamide derivatives using experimental and theoretical tools,

Spectrochim. Acta 224 (2020) 117414.
[74] M. Fleischmann, P.J. Hendra, A.J. McQuillan, Raman spectra of pyridine adsorbed at a silver electrode, Chem. Phys. Lett. 26 (1974) 163–166.
[75] M.G. Albrecht, J.A. Creighton, Anomalously intense Raman spectra of pyridine at a silver electrode, J. Am. Chem. Soc. 99 (1977) 5215–5217.
[76] D.L. Jeanmaire, R.P. Van duyne, Surface Raman spectro electrochemistry, J. Electroanal. Chem. Interfacial Electrochem. 84 (2006) 1–20.
[77] E. Smith, G. Dent, Modern Raman Spectroscopy – A Practical Approach, 2005, https://doi.org/10.1002/0470011831.
[78] K. Kneipp, Y. Wang, H. Kneipp, L.T. Perelman, I. Itzkan, R.R. Dasari, M.S. Feld, Single molecule detection using surface enhanced Raman scattering (SERS), Phys. Rev. Lett. 78 (1997) 1667–1670.
[79] S. Nie, S.R. Emory, Probing single molecules and single nano particles by surface enhanced Raman scattering, Science 275 (1997) 1102–1106.
[80] K.S. Novoselov, A.K. Geim, S.V. Morozov, D. Jiang, Y. Zhang, S.V. Dubonos, I.V. Grigorieva, A.A. Firsov, Electric field in atomically thin carbon films, Science 306 (2004) 666–669.
[81] S. Huh, J. Park, Y.S. Kim, B.H. Hong, J.M. Nam, UV/ozone oxidized large scale graphene platform with large chemical enhancement in surface enhanced Raman scattering, ACS Nano 5 (2011) 9799–9806.
[82] X. Yu, H. Cai, W. Zhang, X. Li, N. Pan, Y. Luo, X. Wang, J.G. Hou, Tuning chemical enhancement of SERS by controlling the chemical reduction of graphene oxide nano sheets, ACS Nano 5 (2011) 952–958.
[83] T. Yu, A. Li, Y. Zhang, Z. Ni, Y. Wang, Z. Zafar, Z. Xiang Shen, T. Qiu, Z. Ni, S. Qu, Surface enhanced Raman scattering of aged graphene:effects of annealing in vacuum, Appl. Phys. Lett. 99 (2011) 233103.
[84] J. Liu, H. Cai, X. Yu, K. Zhang, X. Li, J. Li, N. Pan, Q. Shi, Y. Luo, X. Wang, Fabrication of graphene nanomesh and improved chemical enhancement for Raman spectroscopy, J. Phys. Chem. C116 (2012) 15741–15746.
[85] A.K. Geim, K.S. Novoselov, The rise of graphene, Nat. Mater. 6 (2007) 183–191.
[86] V. Sharma, N.N. Som, S.B. Pillai, P.K. Jha, Utilization of doped GQDs for ultrasensitive detection of catastrophic melamine: a new SERS platform, Spectrochim. Acta 224 (2020) 117352.